A DOUBLY FED INDUCTION GENERATOR CONTROLLED IN SINGLE-SIDED GRID CONNECTION FOR WIND TURBINES

[1]K. RAVI KUMAR, [2]S.VENKATESH

[1,2]Asst.professor, Department of EEE, KKR & KSR Institute of Technology & Sciences, Guntur, A. P., India.
E-mail: [1]ravi1302flux@gmail.com, [2]svraju.260@gmail.com

Abstract- Generally, Wind energy systems are need of the hour from electrical energy system point of view. Doubly fed electric machines are best suited for wind systems due to their ability to work under variable speed conditions in new configuration such as single external feeding of DFIG (SEF-DFIG) which has significant merits over the former system. This paper also proposes the concept of hybrid grid energy system which consists of wind and an ANN controller for controlling the dc-link voltage of SEF-DFIG.. The performance of this hybrid system is observed by simulation case study demonstrate the usefulness of the proposed system.

I. INTRODUCTION

At present, most of energy demand in the world relies on fossil fuels such as petroleum, coal, and natural gas that are being exhausted very fast. One of the major severe problems of global warming is one of these fuels combustion products, carbon dioxide; these are resulting in great danger for life on our planet [1].
Fossil fuels can have as an alternative some renewable energy sources like solar, wind, biomass, and so; among them on the wind energy system which converts the wind energy into electricity, largely used in low power applications. The wind generator is chosen for its positive points including being carbon free and inexhaustible; moreover, it does not cause noise for it is without moving parts and with size-independent electric conversion efficiency [2].

Nevertheless, the power generated by a wind energy system is influenced by weather conditions; for example, at rainy or in cloudy periods, it would not generate any power or application. In addition, it is difficult to store the power generated by a wind system for future use. The best method to overcome this problem is to integrate the wind generator with other power sources such as PV, electrolyzer, hydrogen storage tank, FC system, or battery due to their good features such as high efficiency response, modular production, and fuel flexibility [3, 4]. Its coordination with a wind system could be successful for both grid-connected and stand-alone power applications. Thanks to the rapid response capability of the fuel cell power system, the wind based photovoltaic fuel cell hybrid system can be able to overcome the inconvenience of the intermittent power generation. Hence, the coordination between the FC power system and the photovoltaic generator with wind turbine system becomes necessary in order to smooth out the wind power fluctuations.
This paper focuses on developing a simulation model to design and size the hybrid system for a variety of loading and meteorological conditions. This simulation model is performed using Matlab and SimPower Systems and results are presented to verify the effectiveness of the proposed system. The proposed grid connected hybrid energy generation system is shown in figure 1.

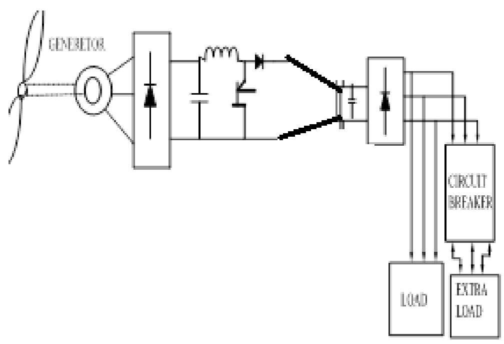

Fig 1: Configuration of proposed grid connected hybrid system

Figure 1 shows the configuration structure for hybrid system based fuel cell, solar and wind energy systems. A rotor in the wind turbine captures the wind's kinetic energy, it consisting of two or more blades mechanically coupled to an electrical generator [4]. The mechanical power captured from wind by a wind turbine can be formulated as:

$$P_m = 0.5 \rho A C_p V^3$$

0.59 is the theoretical maximum value power coefficient value, It is based on two variables the pitch angle tip speed ratio (TSR). With respect to longitudinal axis turbine blades are aligned at an angle that is the pitch angle. The linear speed of the rotor to the wind speed is TSR.

Wind turbine "C Vs. λ" curve is shown in Figure.2. In practical designs, 0.4 to 0.5 is the maximum achievable range for high speed turbines and for slow speed turbines it is in the range of 0.2 to 0.4. At λopt its maximum value (C_{pmax}) is shown in Figure 2. Which results in optimum efficiency and maximum power is captured from wind by the turbine.

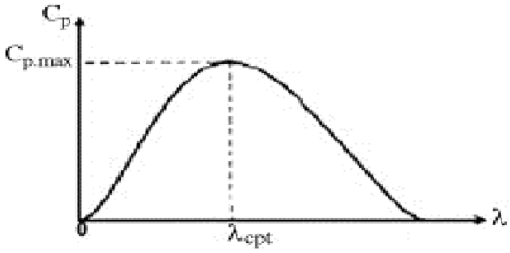

Figure 2: Power coefficient Vs Tip Speed Ratio

II. MODELLING AND DESIGN OF DFIG:

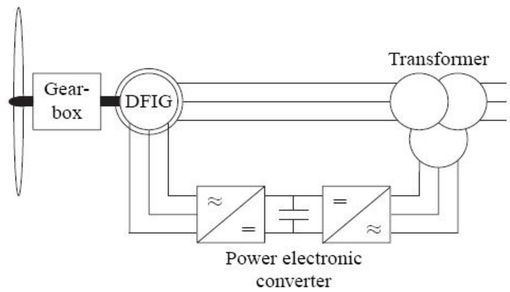

Figure 3: Schematic Diagram for DFIG based wind turbine

Figure 3 shows the schematic diagram of wind turbine based doubly fed induction generator system. The converter in the stator side connected to grid terminals called as Grid controller and rotor converter is act like a feedback converter.

The electrical equivalent circuit of the doubly fed induction generator is shown in Figure 4. In this the stator and rotor windings are simply replaced by resistor and inductor parameters.

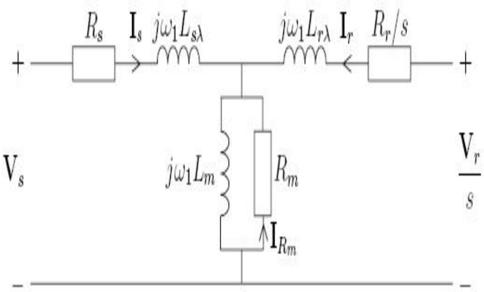

Figure 4: Equivalent circuit of DFIG

From figure shown in 4 the expressions for stator and rotor voltages are written by using Kirchhoff's Voltage Law

$$V_s = j\omega_1 L_m (I_s + I_r + I_{Rm}) + j\omega_1 L_{s\lambda} I_s + R_s I_s \quad (1)$$

$$V_r/s = j\omega_1 L_m (I_s + I_r + I_{Rm}) + j\omega_1 L_{r\lambda} I_r + R_r/s * I_r \quad \text{........} \quad (2)$$

$$0 = j\omega_1 L_m (I_s + I_r + I_{Rm}) + R_m I_{Rm} \quad (3)$$

Rotor flux, stator flux, air-gap fluxes used in equations (1), (2) and (3) are defined below

$$\Psi_m = L_m (I_s + I_r + I_{Rm}) \quad (4)$$

$$\Psi_s = L_{s\lambda} I_s + \Psi_m = L_{s\lambda} I_s + L_m (I_s + I_r + I_{Rm}) \quad (5)$$

$$\Psi_r = L_{r\lambda} I_r + \Psi_m = L_{r\lambda} I_r + L_m (I_s + I_r + I_{Rm}) \quad (6)$$

The electro-mechanical torque is obtained from the above equations is expressed as

$T_e = 3n_p I_m \Psi_r I_r^{*} = 3n_p I_m \Psi_m I^{*}_r$ (7)

Wind-Turbine based doubly fed Induction Generator:

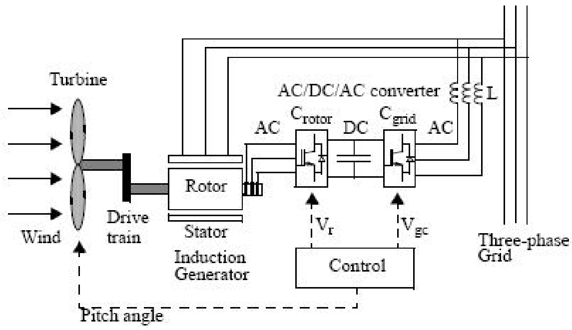

Figure 5: DFIG Connected to Wind Turbine

Basically, the doubly fed induction generator converts mechanical energy which is generated by the wind turbine system into electrical energy. Figure 5 shows the schematic diagram of the doubly fed induction generator based wind turbine system. The control diagram shown in the figure is used for controlling the stator and rotor converters by the reference command signals rotor voltage (V_r) and grid voltage (V_{gc}). And the pitch angle controller is used to change blade positions w.r.t the wind direction.

III. CLOSED LOOP CONTROL DIAGRAM FOR ROTOR SIDE CONTROLLER:

In the RSC, the rotor's active and reactive powers are controlled with the help of rotor flux reference frame axis and voltage signals.

The equations are written by using Kirchhoff's Voltage law for the circuit shown in figure 4.

$$\bar{V}_r = \bar{I}_r R_r + \frac{d\psi_r}{dt} \quad (11)$$

$$\bar{\psi}_r = L_r \bar{I}_r + M\ \bar{I}_s e^{-j\in} \quad (12)$$

Substituting the value of $\bar{\psi}_r$ in above equation e get

$$\bar{V}_r = \bar{I}_r R_r + \frac{d}{dt}(L_r \bar{I}_r + \frac{M}{L_s}\bar{\psi}_s e^{-j\in} - \frac{M^2}{L_s}\bar{I}_r$$

$$= \bar{I}_r R_r + \frac{d}{dt}\left(L_r \bar{I}_r - \frac{M^2}{L_s} \bar{I}_r \right) + \frac{d}{dt}\left(\frac{M}{L_s} \psi_s e^{-j\in} \right)$$

The rotor side converter control structure contains two cascaded loops shown in figure 6. The first loop called as outer loop is used for controlling active and reactive powers of the doubly fed induction generator with reference to the direct and quadrature axis currents. And the second loop is called as inner loop and is used for generating the gate signals to the RSC converter.

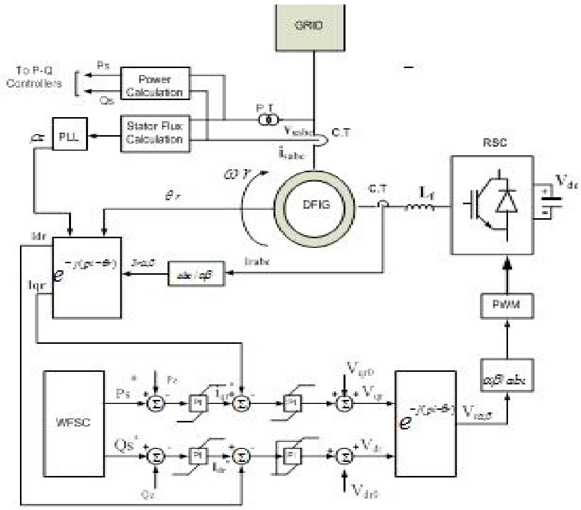

Figure 6: Control Diagram for the rotor side controller

Artificial Neural Networks:

Figure 7 shows the basic architecture of artificial neural network, in which a hidden layer is indicated by circle, an adaptive node is represented by square. In this structure hidden layers are presented in between input and output layer, these nodes are functioning as membership functions and the rules obtained based on the if-then statements is eliminated. For simplicity, we considering the examined ANN has two inputs and one output. In this network, each neuron and each element of the input vector p are connected with weight matrix W.

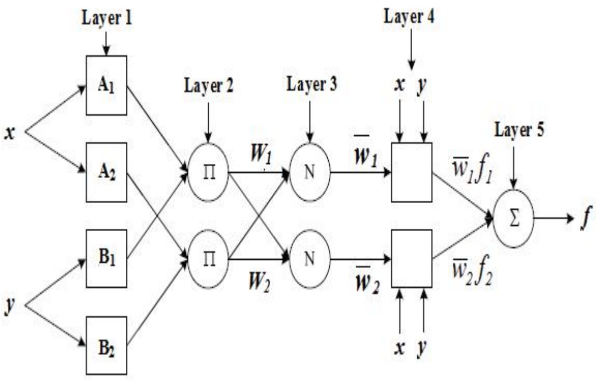

Figure 7 ANN architecture for a two-input multi-layer network

Step by step procedure for implementing ANN:

1. Identify the number of input &outputs in the normalized manner in the range of 0-1.
2. Assume number of input stages.
3. Identify number of hidden layers.
4. By using transig and poslin commands create a feed forward network.
5. Assume the learning rate should be 0.02.
6. Choose the number of iterations.
7. Choose goal and train the system.
9. Generate the simulation block by using 'genism' command

IV. RESULTS AND DISCUSSION

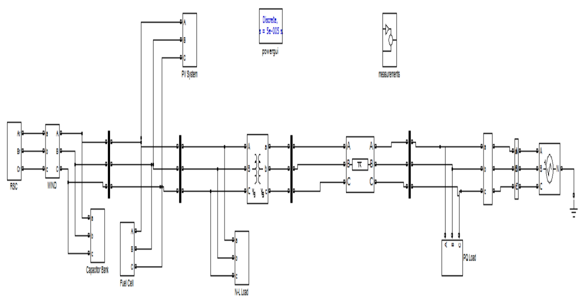

Figure 8 Simulation model of the proposed system

The complete grid connected hybrid system is given in figure 8.

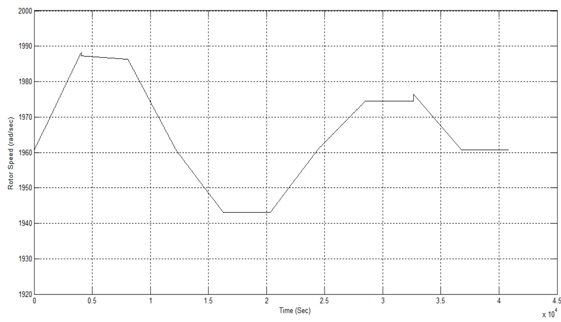

Fig 9: Speed vs time of SEF-DFIG

Figure 9 explains the simulation result for wind turbine speed and it is chosen based on time to time variation. Fig 10 shows the simulation result for three phase voltage and current from the SEF-DFIG structure. Figure 11 is the simulation result for active and reactive powers at grid terminals.

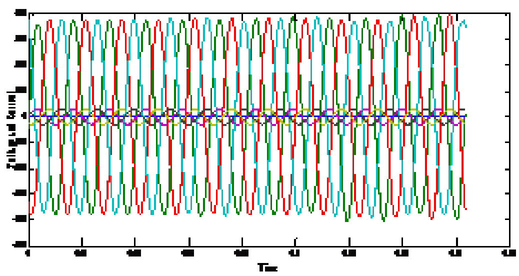

Fig 10: Voltage and Current vs time of SEF-DFIG

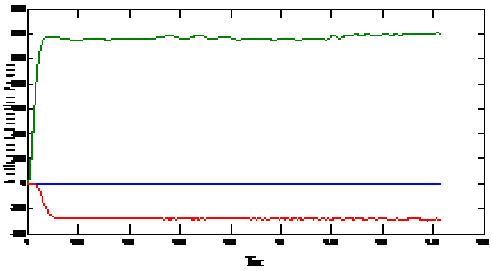

Fig 11: P&Q vs time of SEF-DFIG

Fig 12 are the simulation results which shows the active and reactive powers for grid connected hybrid energy system. And figure 13 and figure 14 shows the results for total harmonic distortions with and without ANN controller.

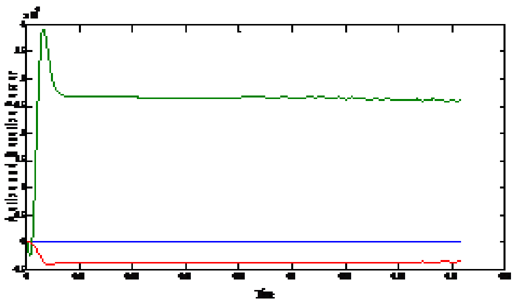

Fig 12: P&Q at the grid terminals when all the sources are connected

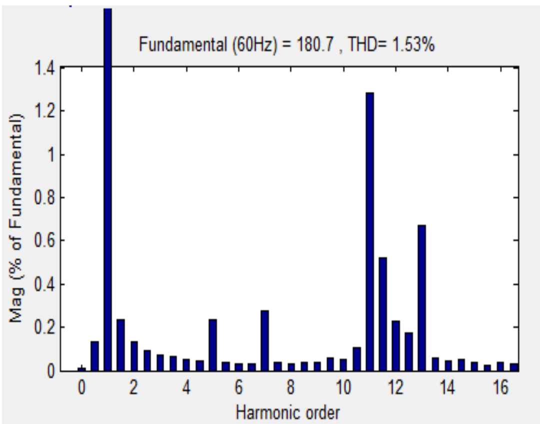

Fig 13: THD for Non-Linear Load current without ANN

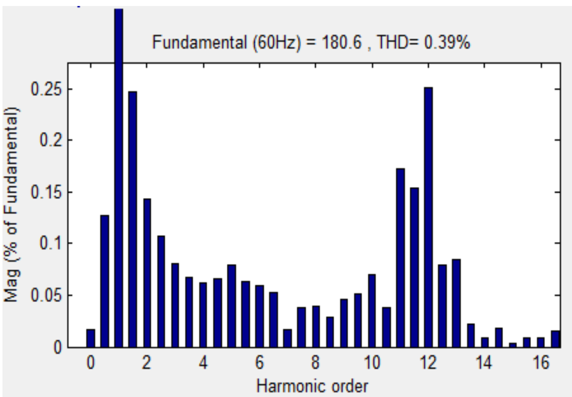

Fig 14: THD for Non-Linear Load current with ANN

CONCLUSION

The effectiveness of isolated power systems are evaluated in MATLAB PC environment. The proposed DFIG configuration is better compared to the conventional configuration with more power output and improved system characteristics. It is observed that the proposed configuration is low cost and having less complexity. The gird is utilized to supply to the unmet power demand by the isolated power systems if they are connected to the gird. On the whole, the performance of isolated system is better and economically beneficial to the customers at large and is very effective for rural areas to meet remote loads.

REFERENCES

[1] R. Datta and V. T. Ranganathan, “Variable-speed wind power generation using doubly fed wound rotor induction machine—A comparison with alternative schemes,” IEEE Trans. Energy Convers., vol. 17, no. 3, pp. 414–421, Sep. 2002.

[2] J. Arbi, M. J.-B. Ghorbal, I. Slama-Belkhodja, and L. Charaabi, “Direct virtual torque control for doubly fed induction generator grid connection,” IEEE Trans. Ind. Appl., vol. 47, no. 1, pp. 4163–4173, Jan./Feb. 2011.

[3] A. Luna, K. Lima, D. Santos, R. Paul, and S. Arnaltes, “Simplified modeling of a DFIG for transient studies in wind power applications,” IEEE Trans. Ind. Electron., vol. 58, no. 1, pp. 9–19, Jan 2011.

[4] M. J. Hossain, H. P. Pota, V. A. Ugrinovskii, and R. A. Ramos, “Simultaneous STATCOM and pitch angle control for improved LVRT capability of fixed-speed wind turbines,” IEEE Trans. Sustainable Energy, vol. 1, no. 3, pp. 142–151, Oct. 2010.

[5] A. Cause brook, D. J. Atkinson, and A. G. Jack, “Fault ride-through of large wind farms using series dynamic braking resistors,” IEEE Trans. Power Syst., vol. 22, no. 3, pp. 966–975, Aug. 2007.

[6] M. E. Haque, M. Negnevitsky, and K. M. Muttaqi, “A novel control strategy for a variable-speed wind turbine with a permanent-magnet synchronous generator,” IEEE Trans. Ind. Appl., vol. 46, no. 1, pp. 331–339,Jan./Feb 2010.

[7] W. Oiao, L. Qu, and R. G. Harley, “Control of IPM synchronous generator for maximum wind power generation considering magnetic saturation,” IEEE Trans. Ind. Appl., vol. 45, no. 3, pp. 1095–1105, May/Jun. 2009.

[8] C. S. Brune, R. Spee, and K. Wallace, “Experimental evaluation of a ´ variable-speed doubly-fed wind-power generation system,” IEEE Trans. Ind. Appl., vol. 30, no. 3, pp. 648–655, May/Jun. 1994.

[9] S. Bhowmik, R. Spee, and J. H. R. Enslin, “Performance optimization ´ for doubly fed wind power generation systems,” IEEE Trans. Ind. Appl., vol. 35, no. 4, pp. 949–958, Jul/Aug. 1999.

[10] C.-H. Liu and Y.-Y. Hsu, “Effect of rotor excitation voltage on steady-state stability and maximum output power of a doubly fed induction generator,” IEEE Trans. Ind. Electron., vol. 58, no. 4, pp. 1096–1109, Apr. 2011.

[11] A. Petersson and S. Lundberg, “Energy efficiency comparison of electrical systems for wind turbines,” in Proc. IEEE Nordic Workshop Power Ind. Electron. (NORPIE), Stockholm, Sweden, Aug. 2002, pp. 12–14.

[12] A. C. Smith, R. Todd, M. Barnes, and P. J. Tavner, “Improved energy conversion for doubly fed wind generators,” IEEE Trans. Ind. Appl., vol. 42, no. 6, pp. 1421–1428, Nov./Dec. 2006.

[13] S. Muller, M. Deicke, and R. W. De Doncker, "Doubly fed induction ¨ generator systems for wind turbines," IEEE Ind. Appl. Mag., vol. 8, no. 3, pp. 26–33, May/Jun. 2002.

[14] G. D. Marques and D. M. Sousa, "Air-gap-power-vector-based sensor less method for DFIG control without flux estimator," IEEE Trans. Ind. Electron., vol. 58, no. 10, pp. 4717–4726, Oct. 2011.

[15] A. Petersson, L. Harnefors, and T. Thiringer, "Evaluation of current control methods for wind turbines using doubly-fed induction machine," IEEE Trans. Power Electron., vol. 20, no. 1, pp. 227–235, Jan. 2005.

[16] L. Gao, B. Guan, Y. Zhou, and L. Xu, "Model reference adaptive system observer based sensorless control of doubly-fed induction machine," in Proc. 2010 Int. Conf. Electr. Mach. Syst., Oct. 2010, pp. 931–936.

[17] L. Xu and W. Cheng, "Torque and reactive power control of a doubly fed induction machine by position sensorless scheme," IEEE Trans. Ind. Appl., vol. 31, no. 3, pp. 636–641, May 1995.

[18] B. Singh, S. K. Aggarwal, and T. C. Kandpal, "DFIG-based wind power conversion with grid power leveling for reduced gusts," IEEE Trans. Sustainable Energy, vol.3, no. 1, Jan. 2012.

[19] L. Qu and W. Qiao, "Constant power control of DFIG wind turbine with super capacitor energy storage," IEEE Trans. Ind. Appl., vol. 47, no. 1, pp. 359–367, Jan./Feb. 2011.

[20] C. Abbey and G. Joos, "Super capacitor energy storage for wind energy applications," IEEE Trans. Ind. Appl., vol. 43, no. 3, pp. 769–776, May/Jun. 2007.

[21] J. Lopez, E. Gubia, E. Olea, J. Ruiz, and L. Marroyo, "Ride through of wind turbines with doubly fed induction generator under symmetrical voltage dips," IEEE Trans. Ind. Electron., vol. 56, no. 10, pp. 4246–4254, Oct. 2009.

[22] J. Morren and S. de Haan, "Ride through of wind turbines with doubly-fed induction generator during a voltage dip," IEEE Trans. Energy Convers., vol. 20, no. 2, pp. 435–441, Jun. 2005.

[23] P. Flannery and G. Venkataramanan, "A fault tolerant doubly fed induction generator wind turbine using a parallel grid side rectifier and series grid side converter," IEEE Trans. Power Electron., vol. 23, no. 3, pp. 1126–1135, May 2008.

[24] P. Flannery and G. Venkataramanan, "Unbalanced voltage sag ride through of a doubly fed induction generator wind turbine with series grid-side converter," IEEE Trans. Ind. Appl., vol. 45, no. 5, pp. 1879– 1887, Sep. 2009.

★★★